Computational investigation of impact energy absorption capability of polyurea coatings via deformation-induced glass transition

M. Grujicic [a,*], B. Pandurangan [a], T. He [a], B.A. Cheeseman [b], C.-F. Yen [b], C.L. Randow [b]

[a] Department of Mechanical Engineering, Clemson University, Clemson, SC 29634, United States
[b] Army Research Laboratory – Weapons & Materials Research Directorate, Aberdeen, Proving Ground, MD 21005-5069, United States

ARTICLE INFO

ABSTRACT

A number of experimental investigations reported in the open literature have indicated that the application of polyurea coatings can substantially improve blast and ballistic impact resistance/survivability of buildings, vehicles and laboratory test plates. While several potential mechanisms (e.g., shock-impedance mismatch, shock-wave dispersion, fracture-mode conversion and strain delocalization) have been proposed for the observed enhancement in the blast-wave/projectile-energy absorption, direct experimental or analytical evidence for the operation of these mechanisms has been lacking. Recently, it has been proposed that transition of polyurea between its rubbery-state and its glassy-state under high deformation-rate loading conditions is another possible mechanism for the improved ballistic impact resistance of polyurea-coated structures/test plates. In the present work, an attempt is made to provide computational support for this deformation-induced glass transition based energy-dissipation/absorption mechanism. Towards that end, a series of finite-element analyses of the projectile/coated-plate interactions are carried out using a transient non-linear dynamics finite-element approach. The results obtained are used to assess the extent of energy absorption and to identify the mode of failure of the test plate as a function of the imposed impact conditions. The results obtained show that the mechanical response of polyurea under impact conditions is a fairly sensitive function of the difference between the test temperature and the glass transition temperature. Specifically, when this difference is large, polyurea tends to display high-ductility behavior of a stereotypical elastomer in its rubbery-state. On the other hand, when the test temperature is closer to the glass transition temperature, polyurea tends to transform into its glassy-state during deformation and this process is associated with viscous type energy-dissipation. It is also argued that additional energy absorbing/dissipating mechanisms may contribute to the superior ballistic/blast protection capability of polyurea.

© 2010 Elsevier B.V. All rights reserved.

1. Introduction

Due to ever-increasing threat to the military personnel and US-owned infrastructure/property around the world, there is an urgent need to develop effective protection methods against bombs, ordnance and Improvised Explosive Devices (IEDs). For example, conventional structures are primarily designed for greater strength and higher serviceability and are hence quite vulnerable to the aforementioned threats. In fact, even conventionally reinforced structures are generally not capable of surviving blast-loads and fragment impacts associated with exploded high-potency IEDs.

One of the newer approaches to countering/mitigating the effects of bombs, ordnance and IEDs, is the application of the elastomeric coatings to the protected structures. The success of this approach was first demonstrated for the case of building walls coated with a few-mm thick layer of polyurea in the early work carried out by the US Air Force [1]. The main role/function provided by the polyurea coating was to contain wall fragments/debrees and prevent them from entering the building interior. These fragments can typically be propelled to a velocity on the order of 100 m/s and are the second-leading cause of injury to the building occupants. In a follow-up investigation, US Navy extended the use of polyurea coatings to enhance the penetration/fracture resistance of its vehicles/structures under the impact by blast-fragments and projectiles [2]. Specifically, the resistance to penetration from gunfire and fragmenting explosives of US Marine Corp's High Mobility Multipurpose Wheeled Vehicle (HMMWV) was substantially improved via coating-based up-armoring of the light tactical military vehicles [3].

* Corresponding author at: 241 Engineering Innovation Building, Clemson University, Clemson, SC 29634-0921, United States. Tel.: +1 864 656 5639; fax: +1 864 656 4435.
E-mail address: mica.grujicic@ces.clemson.edu (M. Grujicic).

1. REPORT DATE **2010**	2. REPORT TYPE	3. DATES COVERED **00-00-2010 to 00-00-2010**

4. TITLE AND SUBTITLE	5a. CONTRACT NUMBER
Computational investigation of impact energy absorption capability of polyurea coatings via deformation-induced glass transition	5b. GRANT NUMBER
	5c. PROGRAM ELEMENT NUMBER

6. AUTHOR(S)	5d. PROJECT NUMBER
	5e. TASK NUMBER
	5f. WORK UNIT NUMBER

7. PERFORMING ORGANIZATION NAME(S) AND ADDRESS(ES) **Clemson University,Department of Mechanical Engineering,241 Engineering Innovation Building,Clemson,SC,29634**	8. PERFORMING ORGANIZATION REPORT NUMBER

9. SPONSORING/MONITORING AGENCY NAME(S) AND ADDRESS(ES)	10. SPONSOR/MONITOR'S ACRONYM(S)
	11. SPONSOR/MONITOR'S REPORT NUMBER(S)

12. DISTRIBUTION/AVAILABILITY STATEMENT
Approved for public release; distribution unlimited

13. SUPPLEMENTARY NOTES

14. ABSTRACT
A number of experimental investigations reported in the open literature have indicated that the application of polyurea coatings can substantially improve blast and ballistic impact resistance/survivability of buildings, vehicles and laboratory test plates. While several potential mechanisms (e.g., shockimpedance mismatch, shock-wave dispersion, fracture-mode conversion and strain delocalization) have been proposed for the observed enhancement in the blast-wave/projectile-energy absorption direct experimental or analytical evidence for the operation of these mechanisms has been lacking. Recently, it has been proposed that transition of polyurea between its rubbery-state and its glassy-state under high deformation-rate loading conditions is another possible mechanism for the improved ballistic impact resistance of polyurea-coated structures/test plates. In the present work, an attempt is made to provide computational support for this deformation-induced glass transition based energy-dissipation/absorption mechanism. Towards that end, a series of finite-element analyses of the projectile/coated-plate interactions are carried out using a transient non-linear dynamics finite-element approach. The results obtained are used to assess the extent of energy absorption and to identify the mode of failure of the test plate as a function of the imposed impact conditions. The results obtained show that the mechanical response of polyurea under impact conditions is a fairly sensitive function of the difference between the test temperature and the glass transition temperature. Specifically, when this difference is large, polyurea tends to display high-ductility behavior of a stereotypical elastomer in its rubbery-state. On the other hand, when the test temperature is closer to the glass transition temperature, polyurea tends to transform into its glassy-state during deformation and this process is associated with viscous type energy-dissipation. It is also argued that additional energy absorbing/dissipating mechanisms may contribute to the superior ballistic/blast protection capability of polyurea.

15. SUBJECT TERMS

16. SECURITY CLASSIFICATION OF:			17. LIMITATION OF ABSTRACT	18. NUMBER OF PAGES	19a. NAME OF RESPONSIBLE PERSON
a. REPORT **unclassified**	b. ABSTRACT **unclassified**	c. THIS PAGE **unclassified**	**Same as Report (SAR)**	**11**	

When testing (experimentally or computationally) the efficacies of various blast/ballistic-mitigation strategies, building walls and vehicle body panels are approximated as thin/thick plate-like structures. There are a relatively large number of reports in the literature concerning the experimental investigations of the structural response of such (non-coated) plates when subjected to impulsive loading. A comprehensive review of these experimental investigations is provided in the work of Nurick and Martin [4] and revealed the use of experimental methods in which the test plate is subjected to air pressure waves created by explosive devices, underwater explosive forming, shock loading by means of metal-foam impacting projectile, and direct impulsive loading using plastic sheet explosives and spring loaded arms. The review of Nurick and Martin also included the main analytical/numerical methods (e.g., momentum conservation approach, eigenvalue expansion methods, and wave form approaches) used to investigate the response of (non-coated) plates under dynamic loading [5–8]. As far as the effect of polyurea coating on the dynamic response of test plates is concerned, the literature overview carried out as part of the present work identified the experimental efforts by Tekalur et al. [9] and Amirkhizi et al. [10] and the computational work by Chen et al. [11].

While these studies clearly revealed the blast-mitigation role of polyurea coatings, the mechanism behind this effect was left unidentified.

In their recent work, Roland et al. [12] showed that polyurea (as well as a number of other elastomers) when used as strike face coating for the steel test plates provided a significant enhancement in the ballistic-penetration resistance of these plates with respect to their impact by a 0.50 caliber steel fragment simulating projectile (FSP). By combining the ballistic impact results with the complementary set of dielectric-spectroscopy results Roland and co-workers [13] arrived at the conclusion that the most plausible mechanism responsible for the observed improvement in ballistic impact resistance of the polyurea-coated steel test plates is a phase transition of the polyurea from the rubbery to the glassy state. Initially, the potential role of hydrogen bonding within polyurea on the improved ballistic resistance was not clear. Subsequent investigation carried out by Roland et al. [12] clearly demonstrated that the role of hydrogen bonding is of a secondary nature and that the ballistic-resistance improvement efficacy of a given elastomeric coating is controlled by the closeness of its glass transition temperature to the test temperature. The main objective of the present work is to provide computational support for the ballistic resistance-improvement mechanism based on the deformation-induced glass transition as proposed by Roland and co-workers [12,13].

Polyureas are a class of microphase-separated and thermoplastically-linked elastomeric co-polymers (the terms '*microphase-separated*' and '*thermoplastically-linked*' will be explained later) that are formed by the rapid chemical reaction between isocyanates (organic chemicals containing isocyanate –N=C=O groups) and amines (organic chemicals containing amine –NH₂ groups). A schematic of the polyurea co-polymerization reaction is shown in Fig. 1 in which symbol R is used to represent an aromatic functional group (e.g. di-phenyl methane) while R' is used to denote an aromatic/aliphatic long chain functional group (e.g. poly-tetramethyleneoxide-di-phenyl). Since the co-polymerization/gel reaction times are typically less than a minute, polyurea synthesis can be achieved under a wide range of temperatures and humidity without significantly affecting material microstructure and properties.

As seen in Fig. 1, the co-polymerization reaction creates urea linkages which are highly polar, i.e., contain centers/poles of negative and positive charge. Also shown in Fig. 1 is that urea linkages together with the R functional groups form the so-called "*hard segments*" within individual polyurea chains. Within the same

Fig. 1. Co-polymerization reaction resulting in the formation of segmented polyurea. To simplify the schematic of the molecular structure, symbols HS (hard segment) and SS (soft segment) are used.

chains, R' functional groups form the so-called "*soft segments*". As a result of strong hydrogen bonding between urea linkages of the neighboring chains (or the neighboring portions of the same chain), hard segments are typically microphase-segregated into the so-called "*hard domains*". An example of the formation of hard domains within polyurea is shown in Fig. 2 using a tapping-mode atomic force micrograph. As shown in this figure, (high glass transition temperature (T_g) and crystallizable [14]) hard domains are present as isolated rod-like entities within the compliant/soft (i.e., low glass transition temperature, T_g) matrix composed of non-phase-segregated hard segments and soft segments. In some cases, hard domains are interconnected forming a contiguous network. Since hydrogen bonding within hard domains provides inter-chain joining, polyureas are often referred to as being thermoplastically cross-linked (in contrast to more commonly covalently cross-linked thermosetting) polymers. Thus, hard domains within polyurea act both as stiff/strong reinforcements and also as inter-chain links. Based on the aforementioned molecular- and domain-level microstructures, polyureas are usually described as microphase-separated and thermoplastically cross-linked elastomers (or nanoscale elastomer-based composites).

Due to their highly complex internal microstructure described above, polyureas display a very broad range of mechanical responses under dynamic loading conditions. The main features of this response can be defined as: (a) a high-level of stress vs. strain constitutive non-linearity, (b) extreme strain-rate (and temperature) sensitivity, and (c) a high degree of pressure dependence.

Since the development of a material model which would accurately and robustly account for all these phenomena is quite challenging, it is no wonder that there is a pronounced scarcity in the polyurea material models and in their parameterization.
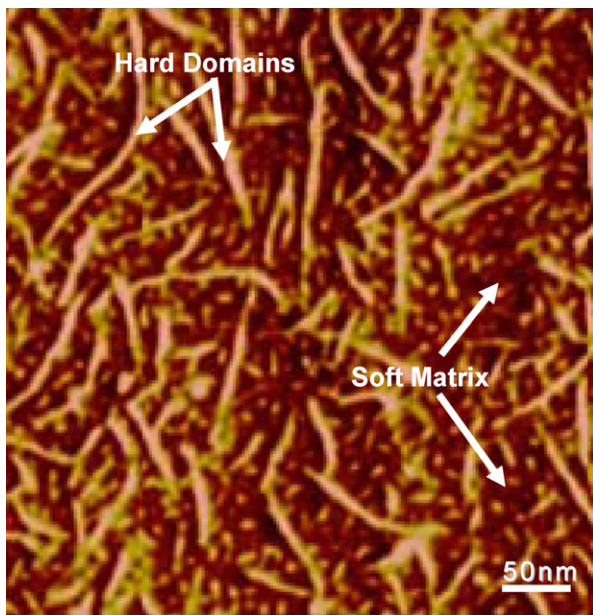
Fig. 2. An example of a typical tapping-mode AFM image of a polyurea showing a rod-like morphology of the hard segments.

A review of the literature carried out as part of the present work revealed the existence of only three material models specifically developed for polyureas [10,15,16].

The first of these models reported in Ref. [10], is an experimentally-based pressure-sensitive linear visco-elastic constitutive model which utilizes the classical Williams–Landel–Ferry (WLF) time–temperature transformation/superposition.

The second model reported in Ref. [15] is of a more complex nature and approximates polyureas as a network of parallel hyperelastic and elastic visco-plastic branches. The hyperelastic branches are modeled using a higher order Ogden strain energy density function while the elastic visco-plastic branches are modeled as collection of springs and dashpots of different stiffnesses and relaxation times. Although this model was found to be relatively successful in reproducing experimental data associated with simple mechanical tests such as uniaxial, plane strain and balanced-by-axial tension/compression, its validity in more general multi-axial stress environments was never demonstrated and the model contains a relatively large number of parameters (many of which have no physical interpretation).

The third model was reported in Ref. [16] and represents a simple superposition of a hyperelastic material model and a non-linear visco-elastic material model. The hyperelastic part of the material model is represented using the Ogden strain energy density function and parameterized using the quasi-static loading stress–strain data. The visco-elastic part of the model, on the other hand, is based on a deformation-history functional and is parameterized using shear-modulus relaxation test data.

An attempt was made in our recent work [17] to remove some of the shortcomings of the three aforementioned material models for polyurea by relating the material response to its molecular/domain-level microstructure. However, only the equilibrium (rate-independent) portion of the material model was developed in Ref. [17]. Since in our prior work [18,19], it was demonstrated that the polyurea material model developed in Ref. [10] yields reasonably good results over a large range of loading rates and stress states, it will be used in the present work.

Polyureas have been used commercially for more than a decade. The most common applications of polyureas include:

(a) Tough, abrasion-resistant, corrosion-resistant, durable and impact-resistant (epoxy/rubber replacement) spray-on coatings/liners in various construction/structural applications such as tunnels, bridges, roofs, parking decks, storage tanks, freight ships, and truck beds,

(b) external and internal wall-sidings and foundation coatings for buildings aimed at minimizing the degree of structure fragmentation and, in turn, minimizing the extent of the associated collateral damage in the case of a bomb blast, and

(c) gunfire/ballistic resistant and explosion/blast mitigating coatings/liners or inter-layers in blast-resistant sandwich panels for military vehicles and structures.

The applications mentioned above capitalize on the exceptional ability of polyureas to alter/disperse shock waves and to absorb the kinetic energy associated with these waves [20] under high-rate loads [21]. As mentioned earlier, Roland and co-workers [13] linked this energy-absorbing capacity of polyurea to its ability to undergo a deformation-induced phase transition during which the rubbery-state of the material is converted to the glassy state. Within the present work, a detailed finite-element analysis of an FSP/coated-plate interaction is carried out in order to provide computational support for the ballistic-resistance improvement mechanism proposed by Roland and co-workers.

The organization of the paper is as follows. A brief description of a typical transient non-linear dynamics problem such as the one dealing with the interactions of an FSP with the test plate is given in Section 2.1. Detailed descriptions of the geometrical and meshed models for the FSP/coated-plate assembly are presented in Section 2.2. A fairly detailed account of the material models assigned to the steel-FSP, the polyurea coating and the steel test plate is provided in Section 2.3. Formulation of the FSP/test-plate interaction problem is presented in Section 2.4. The results obtained in the present work are presented and discussed in Section 3. The main conclusions resulting from the present work are summarized in Section 4.

2. Modeling and computational procedure

2.1. Transient non-linear dynamics analyses of FSP/coated-plate interaction

Within a typical transient non-linear dynamics problem, such as the FSP/coated-plate interaction, an explicit finite-element code (ABAQUS/Explicit [22], in the present work) is employed to solve simultaneously the governing partial differential equations for the conservation of momentum, mass and energy along with the material constitutive equations and the equations defining the initial and the boundary conditions. Such a code typically employs a Lagrangian framework within which the computational finite-element grid is tied to the components/materials (FSP and the coated-plate in the present case) and moves and deforms with them. Within this framework, the aforementioned equations are then solved using a second-order accurate explicit scheme. More details regarding the use of ABAQUS/Explicit in solving transient non-linear dynamics problems can be found in our previous work [23,24].

Within ABAQUS/Explicit, interactions between the FSP and the coated-plate are modeled using the so-called "*Hard Contact Pair*" contact algorithm. Within this algorithm, contact pressures between two bodies (or between two sections of the same body) are not transmitted unless the nodes on the "*slave surface*" contact the "*master surface*". No penetration/over closure is allowed and there is no limit to the magnitude of the contact pressure that could be transmitted when the surfaces are in contact. Transmission of shear stresses across the contact interfaces is defined in terms of a
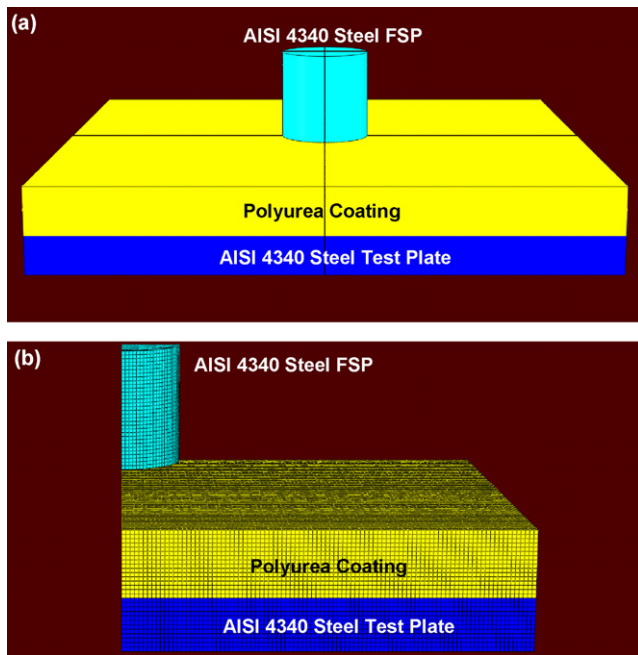
Fig. 3. (a) Geometrical models; and (b) meshed models used in the present work to analyze the interactions of an FSP with a polyurea-coated steel test plate.

Coulomb friction law based on the use of a static and a kinematic friction coefficient and an upper-bound shear stress limit (a maximum value of shear stress which can be transmitted before the contacting surfaces begin to slide).

2.2. Geometrical and meshed models

Since the main objective of the present work was to provide computational support for the ballistic-resistance improvement mechanism associated with polyurea coating of the test plate proposed by Roland and co-workers [13], the computational model was constructed in such a way to closely replicate the experimental set-up used in Ref. [13]. A geometrical representation of the current computational model is given in Fig. 3(a). The model consists of a (12.7 mm diameter, 12.7 mm long) 0.50 caliber right circular solid cylindrical steel-FSP, a (127 mm × 127 mm foot-print) 5.1 mm-thick steel plate top-coated with a 6.4 mm-thick polyurea layer. The FSP, test plate and coating regions are all meshed using first-order, single-integration-point eight-noded elements with a nominal edge length of 0.4 mm. The coating and the test-plate meshes are constructed in such a way that they share all the nodes along the coating/plate interface (i.e., a perfect coating/plate bonding condition is assumed). It should be noted that due to the intrinsic symmetry of the problem, only one-quarter of the FSP/coated-plate assembly is meshed and analyzed, Fig. 3(b). Typically, the meshed model contained between 260,000 and 270,000 finite elements.

2.3. Material models

Since the material constitutive models play a dominant role in transient non-linear dynamics analysis like the one associated with FSP/coated-plate interaction, a detailed account of the constitutive models for the two materials (AISI 4340 steel and polyurea) encountered in the present work is given in this section.

2.4. AISI 4340 steel material model

AISI 4340 steel is modeled as an isotropic, linear elastic and strain-hardenable, rate-dependent, thermally softenable plastic material. Thus the elastic response of this material is defined by two elastic constants (the bulk modulus K and the shear modulus G in the present work). The plastic response of this material is defined by the von-Mises yield criterion, a normality flow-rule and by the Johnson–Cook strain hardening, strain-rate sensitive and pressure softening material constitutive law [25]. Within this model, material yield strength is defined as:

$$Y = \left\lfloor A_1 + B_1 \varepsilon_{pl}^n \right\rfloor \left\lfloor 1 + C_1 \log \dot{\varepsilon}_{pl} \right\rfloor \left\lfloor 1 - T_{HO}^m \right\rfloor \tag{1}$$

where ε_{pl} is the equivalent plastic strain, $\dot{\varepsilon}_{pl}$ the equivalent plastic strain rate, A_1 the zero plastic strain, unit plastic strain rate, room temperature yield stress, B_1 the strain hardening constant, n the strain hardening exponent, C_1 the strain-rate constant, m the thermal softening exponent and $T_{H0} = (T - T_{room})/(T_{melt} - T_{room})$ a room temperature (T_{room}) based homologous temperature while T_{melt} is the melting temperature. All temperatures are given in Kelvin.

Since AISI 4340 steel fails predominantly via a ductile mode, failure of this material is modeled using the Johnson–Cook failure model [26]. The progress of failure according to the Johnson–Cook failure model is defined by the following cumulative damage law:

$$D = \sum \frac{\Delta \varepsilon}{\varepsilon_f} \tag{2}$$

where $\Delta \varepsilon$ is the increment in effective plastic strain with an increment in loading and ε_f, is the failure strain at the current state of loading which is a function of the mean stress, the effective stress, the strain rate and the homologous temperature, given by:

$$\varepsilon_f = \left\lfloor D_3 + D_4 \exp(D_5 \sigma^*) \right\rfloor \left\lfloor 1 + D_6 \ln \dot{\varepsilon}_{pl} \right\rfloor \left\lfloor 1 + D_7 T_{HO} \right\rfloor \tag{3}$$

where σ^* is mean stress normalized by the effective stress. The parameters D_3, D_4, D_5, D_6 and D_7 are all material specific constants. Failure is assumed to occur when $D = 1$.

A summary of the AISI 4340 steel model parameters can be found in Ref. [27].

2.5. Polyurea material model

As mentioned earlier, the mechanical response of polyurea under impact-loading conditions is modeled using a material model reported in Ref. [10]. Since this model was reviewed in great detail in our recent work [18], only a brief summary of it will be provided here. Within the polyurea model used here, the hydrostatic response of the material is considered to be elastic while the deviatoric response of the material is assumed to be time-dependent and hence treated using a geometrically non-linear visco-elastic formulation. Within the hydrostatic part of the model, pressure is defined as a product of a temperature-dependent bulk modulus and a large-deformation volumetric strain. To account for the time-dependent character of the deviatoric material response, the deviatoric stress, σ', at the current time t is evaluated by taking into consideration the entire deformation history of a given material point from the onset of loading at $t = 0$ to the current time as:

$$\sigma'(t) = 2G_\infty \frac{T}{T_{ref}} \int_0^t \left(1 + \sum_{i=1}^n p_i \exp\left(\frac{-\left(\xi(t) - \xi(\tau)\right)}{q_i} \right) D'(\tau) \right) d\tau \tag{4}$$

where G_∞ is the 'long-term' shear modulus (i.e., the value of the shear modulus after infinitely long relaxation time), n is the number of terms in the Prony-series exponential-type relaxation function, p_i and q_i are respectively the strength and the relaxation time of each Prony-series term, ξ is the so-called reduced time

and D' is the deviatoric part of the rate of deformation tensor, D ($D'_{ij} = D_{ij} - 1/3 \times D_{ii}\delta_{ij}$, $i,j = 1$–3, δ_{ij} is the Kronecker delta second-order tensor and summation is implied over the repeated indices). The defining equations for the rate of deformation tensor and for the reduced time can be found in Ref. [10].

A summary of all material model parameters for polyurea can be found in Table 2 of Ref. [18].

2.6. Problem formulation

As mentioned earlier the problem analyzed in the present work deals with the interaction of an FSP with a polyurea-coated steel test plate. The test plate is initially stationary/stress-free and it is simply-supported along all the four back-face edges. The FSP is assigned initially a constant velocity of 900 m/s (selected to match the one used in Ref. [12]). As explained earlier, the FSP/coated-plate contact is handled using the "*hard contact pair*" interaction algorithm. Upon impact, the FSP and the coated-plate begin to deform/fail. Detailed examination of the mechanical response of the polyurea coating is then carried out in order to assess the potential role of the glass transition in enhancing the ballistic protection efficiency of the coating.

3. Results and discussion

3.1. Rubbery-state to glassy-state transition in polyurea

In this section, a brief discussion is provided of the glass transition in polyurea with a particular attention being paid to this transition when occurring under high deformation-rate conditions. As discussed earlier, the defining features of elastomers like polyurea, which govern their engineering application, is the high-level of elasticity and substantial mechanical hysteresis (which imparts high energy absorption capability to this material). However, in some applications such as blast/impact-protective coatings, the mechanical response of the elastomers may be substantially different from the rubber-like behavior discussed above. Specifically, when the loading rates are sufficiently high so that the accompanying strain-rates are comparable with the vibrational frequencies of the chain segments, larger-scale rearrangements of the polymer chains during deformation is precluded. Under such conditions, the elastomer's rubbery-like response becomes more leathery-like, as it transitions to the glassy state. This transition is normally associated with relatively large energy absorption. As clearly articulated by Roland and co-workers [12,13], to fully exploit this phenomenon in blast/impact-protective elastomeric coatings, the (calorimetric) glass-transition temperature, T_g, of the elastomer should be relatively high but lower than the service temperature (with an optimal value of T_g being controlled by the attendant deformation-rate).

Glass transition is a second-order phase transition during which the first-order derivatives of the Gibbs free-energy (e.g. volume, entropy, enthalpy) remain constant while second-order derivatives (e.g. specific heat, coefficient of thermal expansion) undergo a discontinuous change. During cooling, glass transition occurs at a (weakly cooling-rate dependent) temperature, the so-called "*calorimetric glass transition*" temperature. At the molecular-level, the rubbery-state to glassy-state transition is associated with the loss of mobility of the local chain segments. This mobility loss can occur during deformation at temperatures higher than T_g. Consequently, one can define a deformation-rate dependent "*dynamic glass transition*" temperature, as a temperature at which the local segmental dynamics becomes comparable with the imposed deformation-rate. Under such conditions, large viscous type energy-dissipation effects are expected. On the other hand, when the imposed deformation-rate is too low compared to the

local chain dynamics, the elastomeric material will respond in a rubber-like fashion and, due to large-scale mobility of the chain segments based on correlated conformational transitions of a couple of backbone bonds, store (and to a lesser extent dissipate) elastic strain energy. In the other limit when the imposed deformation-rate is too high, the elastomeric material (due to "*frozen-state*" of the chain segments) will behave as a glass and would display little ductility and energy absorption capability.

To determine the local segmental dynamics, i.e., the frequency of the local segmental relaxation processes, Roland and co-workers [13] carried out a comprehensive set of dielectric-spectroscopy/relaxation measurements over a range of temperatures (between the calorimetric T_g and the room temperature) on polyurea. The results obtained revealed the existence of a broad glass-transition peak (the peak half-height half-breadth at the low frequency side being ca. two decades). The unusually large breadth of the glass transition (also often referred to as "*alpha relaxation*") in polyurea is a consequence of the highly complex molecular/domain-level material microstructure as discussed earlier. Roland and co-workers [13] next fitted the frequency associated with the maximum in the dielectric loss at different temperatures, f_{max}, to the Vogel–Fulcher equation in the form:

$$\log f_{max} = \log f_0 - \frac{B \log(e)}{T - T_0} \tag{6}$$

where f_0 (=$11.0 \pm 0.3 \text{ s}^{-1}$) is the asymptotic high temperature value of f_{max} and B (=694 ± 68), T_0 (=160 ± 4.0) are constants, and computed the associated (temperature-dependent) activation energy and found that its value is around 115 kJ/mol at room temperature. At the same temperature, the frequency associated with the maximum in the dielectric loss was found to be ca. 9×10^5 Hz.

In the FSP/coated-plate interaction portion of their work, Roland and co-workers [13] estimated that the average strain-rate within the polyurea coating is around 1.5×10^5 Hz. Roland and co-workers [13] next used the fact that this deformation-rate is only six times smaller than segmental frequency associated with maximum dielectric loss to explain the observed glass-like mode of failure and the associated high energy absorption capability of polyurea.

To further support their hypothesis of deformation-induced glass transition energy absorption enhancement, Roland and co-workers [13] also tested a polybutadiene coating in which the frequency associated with the maximum in the dielectric loss was more than three orders of magnitude higher than the deformation-rate. In this case, the coating remained ductile during impact with the FSP while the associated energy absorption was around two orders of magnitude smaller than in the polyurea case.

3.2. Analysis of the polyurea material model reported in Ref. [10]

As mentioned earlier, the material model for polyurea reported in Ref. [10] is used in the present work. In accordance with Eq. (4) the visco-elastic part of the material model is handled using a four-term Prony-series. Polyurea material model parameterization reported in Table 2 shows four distinct visco-elastic relaxation times, q_i ($i = 1, 4$): 0.4634 s, 6.41×10^{-5} s, 1.163×10^{-7} s and 7.321×10^{-10} s. Using the standard relationship between the frequency associated with the maximum dissipation, f_{max}, and the corresponding relaxation time, $f_{max} = (2\pi q)^{-1}$, the corresponding four f_{max} values are found to be 0.343 Hz, 2.48×10^3 Hz, 1.37×10^6 Hz and 2.17×10^8 Hz, respectively. Examination of these results, and their comparison with the frequency associated with the maximum dielectric loss (9×10^5 Hz), suggests that the third term in the Prony-series, with $f_{max} = 1.37 \times 10^6$, is most likely associated with the rubbery-state to glassy-state transition.

Roland and co-workers [13] clearly articulated the importance of the temperature dependence of the visco-elastic relaxation fre-
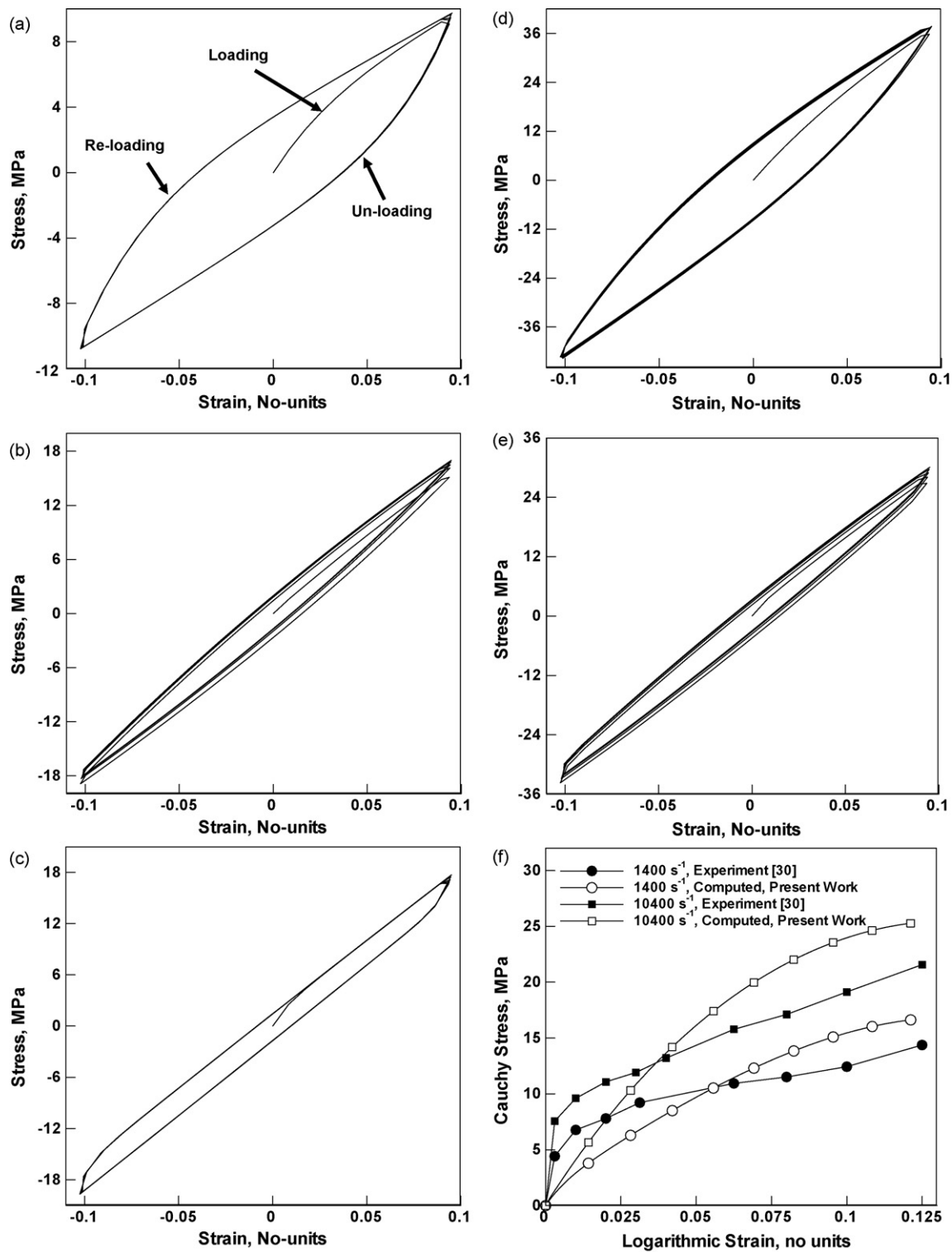
Fig. 4. Balanced-uniaxial cyclic stress–strain curves for polyurea at room temperature at constant engineering strain-rates of (a) $500\,s^{-1}$, (b) $5000\,s^{-1}$, (c) $50,000\,s^{-1}$, (d) $500,000\,s^{-1}$, and (e) $5,000,000\,s^{-1}$. Experimental validation of the present polyurea material model for the case of uniaxial compression initial loading stress vs. strain curve.

quencies and its role in the polyurea's ability to absorb/dissipate energy. It should be noted at this point that in a real polyurea material, the relaxation times and the associated maximum-loss frequencies are temperature sensitive quantities. However, in the polyurea material model reported in Ref. [10], only constant Prony-series parameters are used. These parameters are associated with a master relaxation curve at the (reference) 273 K temperature. The effect of temperature is handled using the

Williams–Landle–Ferry time–temperature superposition principle which effectively replaces the time with a so-called "*reduced-time*". In this way, time is extended at higher temperatures to account for the associated larger extent of relaxation. This is mathematically equivalent to introducing temperature-dependent Prony-series parameters while using the real time. Thus the polyurea material model presented in Ref. [10] can be used to assess the ability of polyurea to absorb/dissipate energy under different loading
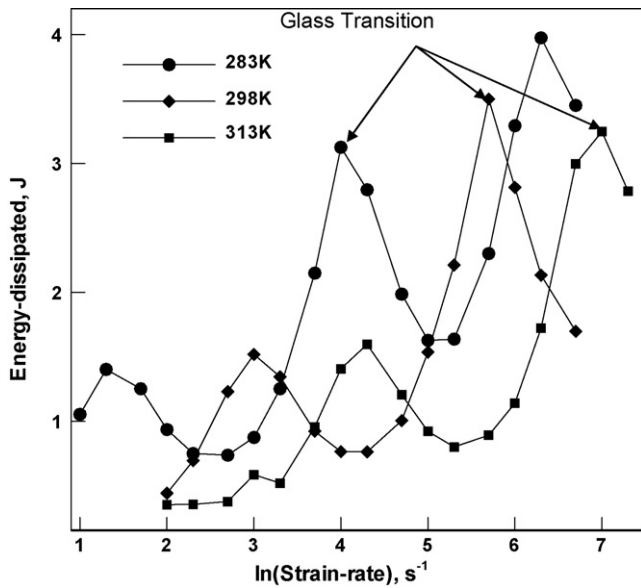
Fig. 5. The effect of test temperature and the imposed uniaxial cyclic engineering strain-rate on the energy absorption capability of polyurea for the −0.10 to 0.10 engineering strain range.

rate/temperature conditions. This was done in the remainder of this section.

An example of the typical cyclic uniaxial stress vs. strain results obtained in the present work is displayed in Fig. 4(a–e). All the results displayed in these figures were obtained at room temperature while the engineering strain-rate (kept constant within a given test) was varied between different tests in a range between $5 \times 10^2 \, s^{-1}$ and $5 \times 10^6 \, s^{-1}$. The results displayed in these figures show that after a couple of cycles a steady/stable stress–strain hysteresis is formed (the area associated with the hysteresis being a measure of the extent of the visco-elastic energy-dissipation). Also the results displayed in Fig. 4(a–e) show that the extent of energy-dissipation is a function of the imposed strain-rate.

To validate the material model used in the present work, a comparison is provided in Fig. 4(f) between Cauchy (true) stress vs. logarithmic strain results predicted by the present model and their experimental counterparts obtained in Ref. [30]. The comparison given in Fig. 4(f) could be carried out only for the loading portions of the stress vs. strain curves since the unloading curves were not generated in Ref. [30], in the strain-rate range of interest in the present study. The results displayed in Fig. 4(f) show that the overall agreement between the computed and the measured stress vs. strain curves is only fair. However, it should be recalled that the material model adopted in the present work was parameterized using (and is in a substantially better agreement with) a separate set of experimental results obtained in Ref. [10]. This finding reiterates the well-known high sensitivity of polyurea properties to variations in its chemistry/stoichiometry, synthesis conditions and microstructure.

To further demonstrate the point that the extent of energy-dissipation is a function of the imposed strain-rate, the energy loss associated with uniaxial cycling between engineering strains of −0.10 and 0.10, as a function of the logarithm of the engineering strain-rate is displayed in Fig. 5. It should be noted that this figure does not only contain the room (298 K) temperature results but also the ones generated at 283 K and at 313 K (i.e., at temperatures which are 15° below and above the room temperature, respectively). To facilitate interpretation of the results displayed in this figure, the energy absorption peak associated with the glass transition is marked for each of the three temperatures.

An examination of the results displayed in Fig. 5 reveals that:

(a) An increase in the test temperature causes an increase in the strain-rate associated with the maximum glass-transition based energy absorption/dissipation. This finding is consistent with the temperature dependence of the dielectric frequency associated with the maximum dissipation reported by Roland and co-workers [13];

(b) the apparent activation energy associated with the glass transition temperature at room temperature is calculated using the results displayed in Fig. 5 and the formula $\Delta G = -R \, \mathrm{d} \ln \dot{\varepsilon}/\mathrm{d}(1/T)$ where R is the universal gas constant; $\dot{\varepsilon}$ the engineering strain-rate and T the temperature. The room temperature value obtained, ca. 120 kJ/mol is quite comparable with its dielectric-relaxation counterpart reported by Roland and co-workers [13]. This finding supports the initial contention made in the present paper that the third Prony-series term in the polyurea material model reported in Ref. [10] is indeed associated with glass transition;

(c) the effect of the difference between the test temperature and the glass transition temperature on the elastomer energy-absorbing capability is also seen in Fig. 5. For example, at an engineering strain-rate of $5 \times 10^5 \, s^{-1}$, highly pronounced energy absorption is seen for the test temperature of 298 K. A change in the test temperature of only 15 K in either direction is seen to substantially reduce the viscous energy-dissipation ability of polyurea. This finding is also fully consistent with that of Roland and co-workers [13]. It should be noted that Roland and co-workers [13] varied the difference between the test temperature and the glass transition temperature by choosing elastomers with different glass transition temperatures (e.g., polybutadiene and polyurea). In the present work, on the other hand, this difference was varied within the same elastomer (polyurea) by changing the test temperature.

It would be helpful, at this point, to provide some experimental validation for the results displayed in Figs. 4(a–e) and 5. As far as the cyclic stress vs. strain results as the ones displayed in Fig. 4(a–e) are concerned, they are usually generated experimentally using Dynamic Mechanical Analysis (DMA). However, DMA is normally limited to loading frequencies under ca. 100 Hz whereas the lowest frequency analyzed in the present work is 500 Hz. While this limitation of the DMA is typically overcome by changing the test temperature and invoking the time–temperature-superposition principle, the relevant DMA results for polyurea are not currently available. Hence, no direct validation of the results displayed in Fig. 4(a–e) can be provided. An indirect validation, however, stems from the fact that the results displayed in Fig. 4(a–e) are obtained using the material model which was based on the monotonic-loading experimental data pertaining to the same strain range [10]. Regarding the validation of the results displayed in Fig. 5, the ones associated with the glass-transition process are found to be in broad quantitative agreement with (i.e., 20–30%) of the dielectric-spectroscopy energy-dissipation results reported by Roland et al. [12].

3.3. Coated test-plate impact and penetration analysis

In their work pertaining to the FSP impact of coated steel test plates, Roland and co-workers [13] used both Polybutadiene (T_g = 182 K and, hence, a large difference between the test temperature and the glass transition temperature) and polyurea (T_g = 213 K and, hence, a smaller difference between the test temperature and the glass transition temperature) as coating materials. When tested under identical FSP impact conditions, they found markedly different response of the two coated test plates. Specifically, in the
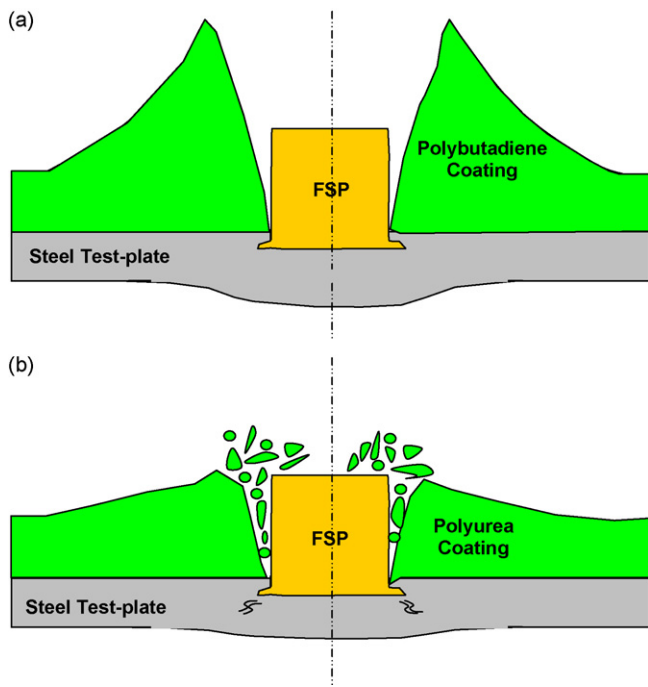
Fig. 6. A schematic of the mechanical response of the coating and the test plate to impact by an FSP: (a) polybutadiene coating; (b) polyurea coating.
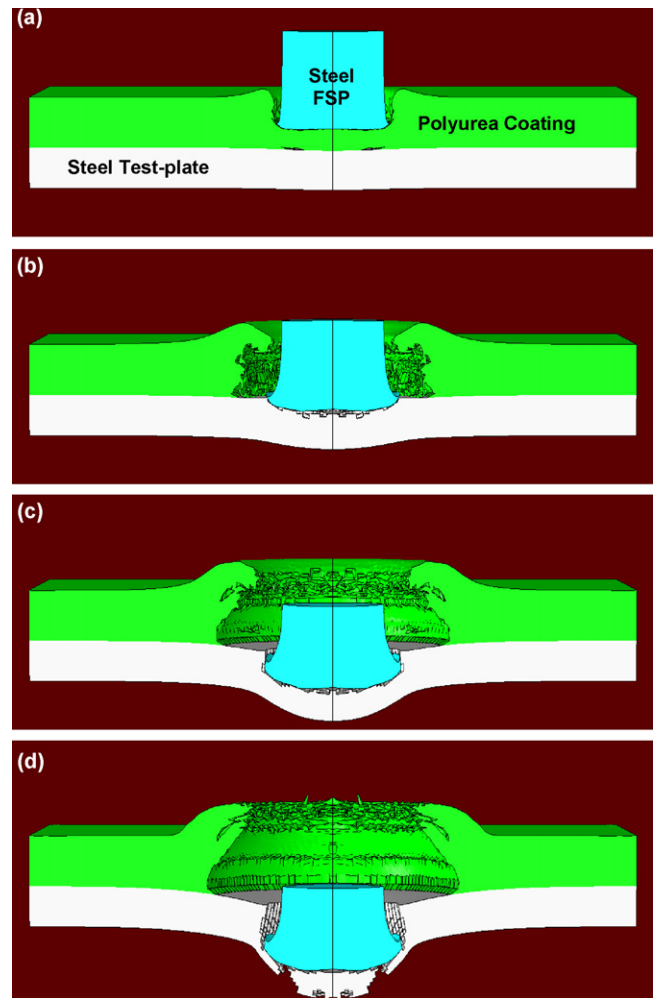

Fig. 7. Temporal evolution and spatial distribution of the materials in the steel-FSP/polyurea coated-plate assembly for the 313 K test-temperature case at the post-impact times of: (a) 5 μs, (b) 12 μs, (c) 21 μs and (d) 30 μs.

case of polybutadiene coating, a fairly normal rubbery response was observed which involved a large-scale/de-localized high-strain deformation mode. In sharp contrast, in the case of polyurea, deformation was found to be highly localized into a narrow region adjacent to the circumferential surface of the projectile and in the region between the projectile and the test plate. The mechanical response of polyurea in the affected regions appeared to be brittle resulting in the formation of a large number of glassy fragments. However, the energy absorption/dissipation was greatly increased relative to that found in the case of highly ductile polybutadiene coating. Due to copyright restrictions the relevant high-speed camera photographs generated in the work of Roland and co-workers [13] could not be reproduced here. Instead a schematic of the response of polybutadiene-coated and polyurea-coated steel test plates under identical FSP impact conditions is depicted in Fig. 6. It is apparent that under the FSP impact conditions in question polyurea was transformed from its rubbery to its glassy-state and that, subsequently, the brittle glassy-state underwent large-scale fragmentation. In the remainder of this section, the finite-element results generated in order to support this hypothesis are presented and discussed.

Temporal evolution and the spatial distribution of the materials within the FSP/coated-plate assembly in the case of: 900 m/s FSP initial velocity, polyurea coating and 313 K test-temperature (the highest test-temperature investigated in the present work) is given in Fig. 7(a–d). A brief examination of the results displayed in Fig. 7(a–d) show that, under the given impact conditions, polyurea behaves as a fairly stereotypical elastomeric material in its rubbery-state. That is, FSP impact onto the coated test-plate results in large-scale and extensive deformation of the coating. This is, in turn, associated with relatively large stored elastic strain energy. The extent of viscous energy-dissipation, on the other hand, is controlled by the closeness of the local deformation-rate and the frequency associated with maximum mechanical-energy loss.

When the same analysis was repeated at 298 K and 283 K test-temperatures, similar material spatial distribution and temporal evolution results (not shown for brevity) as those displayed in

Fig. 7(a–d) were obtained. It should be noted that, in the 298 K case, the observed highly ductile behavior of polyurea is in sharp contrast with the experimental observations (pertaining to brittle-like behavior of polyurea) made by Roland and co-workers [13]. This discrepancy will be discussed in more depth later in this section.

The computational analysis which produced the results displayed in Fig. 7(a–d) (and the corresponding 298 K and 283 K results), also yielded the results pertaining to the associated temporal evolution of the FSP residual velocity. The latter results are displayed in Fig. 8 for the three test temperatures. It is seen that at the intermediate temperature of 298 K, the FSP residual velocity is the lowest. This finding confirms the existence of an optimal test temperature at which the glass-transition based energy losses are the highest. However, the overall difference in the reduction in the projectiles' kinetic energy is fairly small between the three test temperatures investigated.

As mentioned above, the present finite-element investigation initially failed to reproduce brittle-like response of the polyurea coating at room (298 K) temperature as observed in the experimental work of Roland and co-workers [13]. To obtain this type of response of polyurea, it was found necessary to make modifications in the material model reported in Ref. [10]. Specifically, it was found necessary to introduce a fracture (equivalent) strain to account for cracking and fragment formation of the polyurea glassy-state. It should be noted that such a strain was used already in conjunction
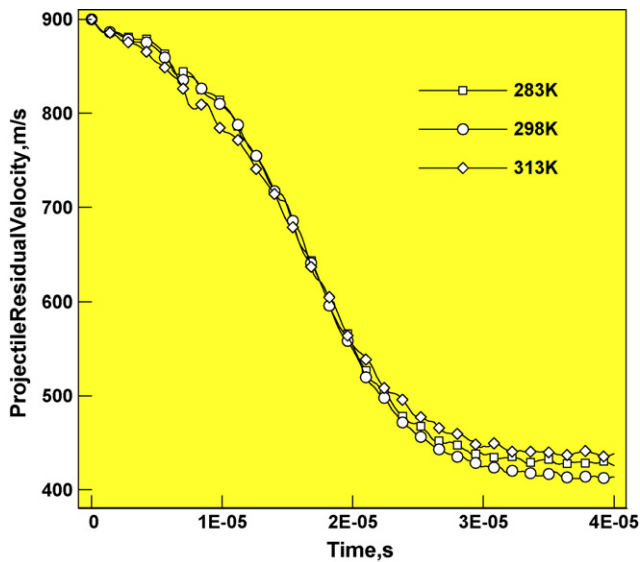
Fig. 8. Temporal evolution of the FSP velocity during the steel-FSP/polyureacoated-plate interaction for the three test temperatures considered in the present work. A constant fracture strain of 3.0 was used at each test temperature.

with results displayed in Fig. 7(a–d) in order to surmount numerical challenges associated with highly distorted polyurea elements. However, the fracture strain was set (arbitrarily) to a relatively large value of 3.0 so that deletion of a relatively small number of "*failed elements*" did not significantly affect the results. To obtain qualitatively similar results to those reported by Roland and co-workers [13] at room (298 K) temperature, the fracture strain had to be set to a value between 1.0 and 2.0 (1.5 in the present work). The major reduction in the fracture strain (from 3.0 to 1.5) between the test temperatures of 313 K and 298 K is consistent with the expected change in the polyurea response from highly ductile to brittle-like.

Temporal evolution and the spatial distribution of the material within the FSP/coated-plate assembly in the case of: 900 m/s FSP initial velocity, polyurea coating and 298K test temperature is given in Fig. 9(a–d). A brief examination of the results displayed in Fig. 9(a–d) shows that:

(a) due to a lower value of the fracture strain, considerable polyurea element deletion has taken place. In the real material, deleted elements would be represented by material fragments. Unfortunately, fragment formation during fracture is beyond the scope of the present work and could not be displayed. An attempt will be made in our future work to incorporate fragment formation following the approach employed in the case of soda-lime glass [28,29],

(b) the deleted elements (fragments) were located in a region adjacent to the circumferential surfaces of the projectile and in the region between the projectile and the test plate. These findings are fully consistent with the results obtained in the experimental work reported by Roland and co-workers [13], and

(c) due to element deletion, the contact-time/area between the FSP and the coating is reduced substantially in the present computational analysis, making the FSP velocity vs. time results less reliable. In other words, while the glassy-polyurea fragments continue to exert normal and tangential forces on the advancing FSP under laboratory test conditions, this effect could not be accounted-for in the present computational analysis.

Temporal evolution and the spatial distribution of the material within the FSP/coated-plate assembly in the case of: 900 m/s FSP initial velocity, polyurea coating and 283 K test temperature is given
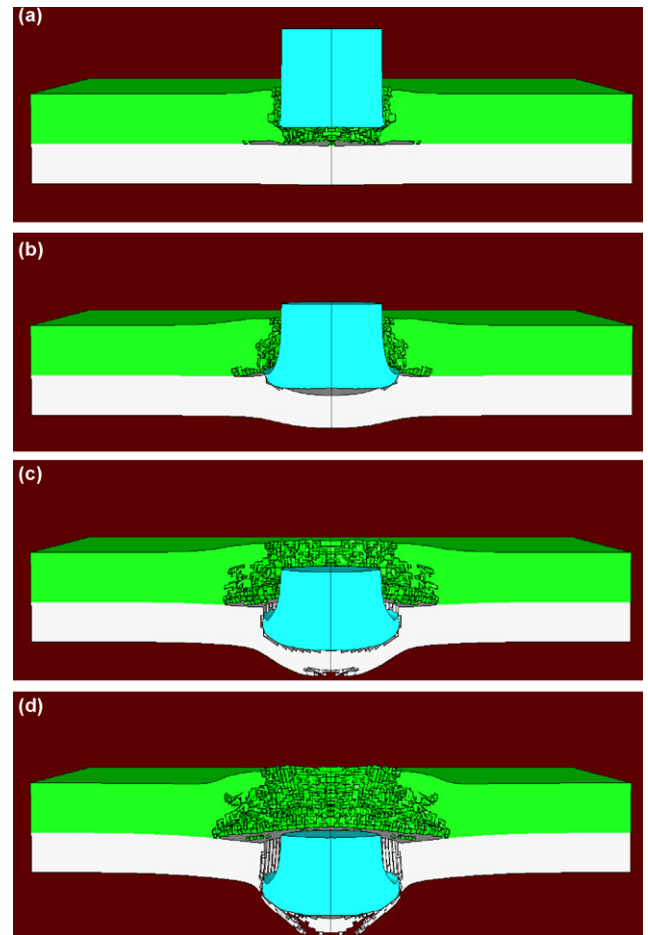
Fig. 9. Temporal evolution and spatial distribution of the materials in the steel-FSP/polyurea coated-plate assembly for the 298 K test-temperature case at the post-impact times of: (a) 5 μs, (b) 12 μs, (c) 21 μs and (d) 30 μs.

in Fig. 10(a–d). It should be noted that an even lower fracture strain of 0.5 was used in this case. A brief examination of the results displayed in Fig. 10(a–d) shows that the regions of deleted elements have been enlarged compared to the 298 K test-temperature case. This finding simply suggests that at the lowest test-temperature examined, the un-stressed polyurea is in a leathery state (a transition state between the rubbery and the glassy states). Hence, under laboratory (283 K) impact-loading conditions, polyurea coating is expected to behave as a brittle-material and to undergo large-scale fracture (and possibly form large fragments). Under these conditions, the ability of polyurea to store/dissipate energy is reduced. However, as pointed out earlier, since the present computational approach does not explicitly account for the polyurea fragmentation process and the interactions between polyurea fragments and the FSP, an accurate assessment of the energy absorbing/storing capacity of polyurea could not be made. Nevertheless, the temporal evolution of the FSP residual velocity for the three test temperatures and the aforementioned temperature-dependent fracture strains are computed and shown in Fig. 11. It is seen that at the intermediate temperature of 298 K, the FSP residual velocity is still the lowest and that the difference between this residual velocity and the other two is somewhat larger than in the case of Fig. 8. However, the overall reduction in the projectile's residual velocity is only 15–20% of that found in the experimental work of Roland and co-workers [13]. A comparison of the results displayed in Figs. 8 and 11 show that the 313 K curves are identical and that a (3.0–1.5) reduction in the fracture strain has resulted in a reduction of the FSP residual velocity in the 298 K case. This finding which sug-
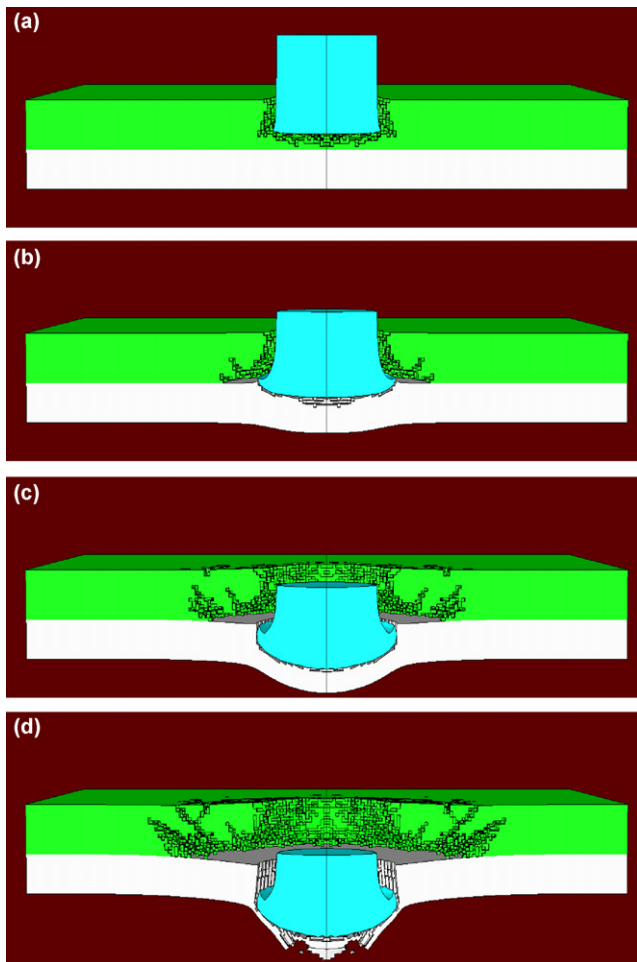
Fig. 10. Temporal evolution and spatial distribution of the materials in the steel-FSP/polyurea coated-plate assembly for the 283 K test-temperature case at the post-impact times of: (a) 5 μs, (b) 12 μs, (c) 21 μs and (d) 30 μs.
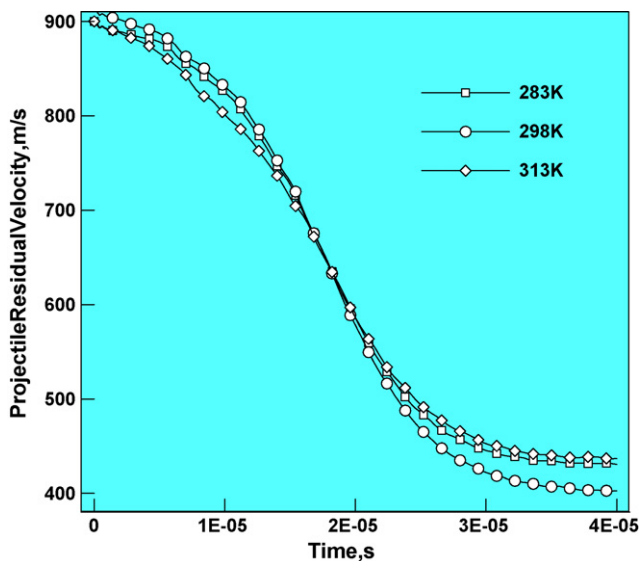

Fig. 11. Temporal evolution of the FSP residual velocity during the steel-FSP/polyurea coated-plate interaction for the three test temperatures considered in the present work. Fracture strains have been selected as: 3.0 at 313 K, 1.5 at 298 K and 0.5 at 283 K.
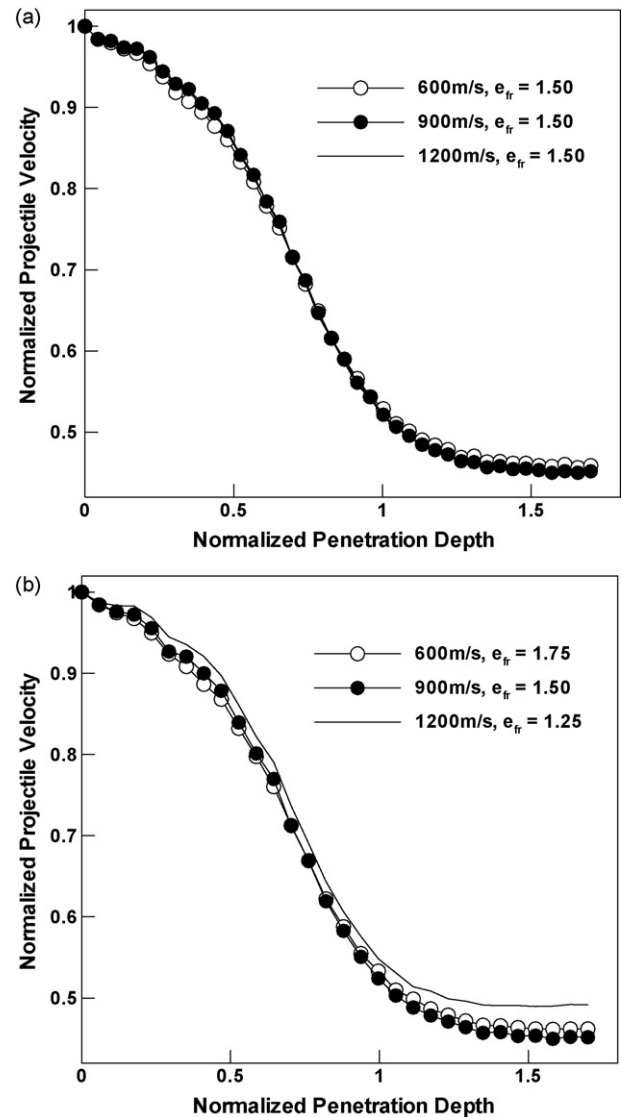

Fig. 12. Variation of the normalized projectile velocity (i.e. projectile velocity divided by the projectile initial velocity) with normalized penetration depth (i.e. a ratio of the penetration depth and the target thickness) at 298 K for three projectile initial velocities and: (a) the case of a constant (1.5) fracture strain; and (b) the case of a strain-rate dependent fracture strain.

gests that a less-ductile equal-strength material may act as a more effective target may not be very intuitive. A close examination of the results obtained revealed that in the case of 3.0 fracture strain, the strain field is more de-localized, the associated strain-rates lower and the extent of strain-rate/segmental frequency-matching less pronounced than in the 1.5 fracture strain case. Consequently, despite its lower ductility, the material in the 1.5 fracture strain case is capable of dissipating more of the projectile kinetic energy.

It should be recalled that the main objective of the present work was to provide computational support for the deformation-induced glass transition in polyurea under impact-loading conditions and for the associated increase in the ballistic/blast protection efficiency of polyurea coatings. The results presented in this section clearly showed that a transition in the polyurea state from rubbery to a deformation-induced glassy state is beneficial from the standpoint of viscous type energy-dissipation. However, the same results suggested that there are additional phenomena such as glassy-polyurea fragmentation and the interaction of the polyurea fragments with FSP which must be taken into account in order to

obtain a more comprehensive insight into the complex nature of FSP/coated-plate interactions. Hence, the future polyurea material modeling and FSP/coated-plate impact simulation efforts should be directed towards including these additional phenomena. Also, it should be recognized that the polyurea material model used in the present work was based on the experimental results covering a range of strains up to 0.4 and showing a good agreement with these results up to a strain of 0.1–0.15 [10]. Hence, the future efforts should also be directed towards upgrading this model to cover a larger strain range. This is the subject of our ongoing investigation.

The computational results presented so far in this section were obtained under the FSP initial-velocity condition of 900 m/s. This was done in order to be able to carry out direct comparison between the computed results obtained in the present work and the corresponding experimental results obtained in the work of Roland and co-workers [13]. Per suggestion of one of the reviewers of the present manuscript, FSP/coated-plate interactions are also analyzed, at room temperature, under a lower (600 m/s) and a higher (1200 m/s) FSP initial velocity. An example of the typical results obtained in this portion of the work is displayed in Fig. 12(a and b). To show the extent of projectile-energy absorption by the target, a normalized projectile velocity (i.e. projectile velocity divided by the projectile initial velocity) is plotted against a normalized penetration depth (i.e. a ratio of the penetration depth and the target thickness) in Fig. 12(a and b). In Fig. 12(a), temporal evolution of the FSP velocity at 298 K is shown for 600 m/s, 900 m/s and 1200 m/s projectile initial-velocity cases while the fracture strain is kept constant (=1.5). It is seen that no significant differences in the relative projectile-energy absorption exist in the 600–1200 m/s projectile-velocity range. Since an increase in the strain-rate is often assumed to have a similar effect on the materials mechanical response as the reduction in temperature, one can assume that the fracture strain is not only temperature but also strain-rate dependent. To examine the potential effect of a strain-rate dependent fracture strain on the projectile residual velocity, fracture strains of 1.75, 1.5 and 1.25 are arbitrarily assigned to the polyurea coating at 298 K when subjected to an FSP impact at an initial velocity of 600 m/s, 900 m/s and 1200 m/s, respectively. The projectile-velocity results obtained in this case are displayed in Fig. 12(b). It is seen that the introduction of a strain-rate dependent 298 K fracture strain can make the extent of projectile-energy absorption more dependent on the projectile initial velocity. In addition, it appears that there is an optimal level of the fracture strain at a given test temperature which is associated with the maximum extent of the projectile-energy absorption.

4. Summary and conclusions

Based on the results obtained in the present work, the following main summary remarks and conclusions can be drawn:

1. One of the available high deformation-rate, large-strain, high-pressure material models for polyurea has been appropriately upgraded to include the effect of fracture and used in a transient non-linear dynamics analysis of impact of a polyurea-coated steel plate by a steel fragment simulating projectile (FSP).
2. The results obtained show that the mechanical response of polyurea under impact conditions is a fairly sensitive function of the test temperature (or more precisely of the difference between the test temperature and the glass transition temperature). Specifically, at higher test temperatures, polyurea tends to display high-ductility behavior of a stereotypical elastomer in its rubbery-state. On the other hand, at lower temperatures (which are still above the glass transition temperature) polyurea tends to transform into its glassy-state during deformation and this process is associated with viscous type energy-dissipation.

3. The computed levels of viscous type energy-dissipation are found to be relatively small compared to the ones reported in the literature. This discrepancy has been discussed in light of the limitations of the computational procedure employed in the present work and in terms of the additional energy absorbing/dissipating mechanisms attending the FSP/coated-plate interaction process.

References

[1] J.R. Porter, R.J. Dinan, M.I. Hammons, K.J. Knox, AMPTIAC Quart. 6 (4) (2002) 47–52.
[2] S.A. Tekalur, A. Shukla, K. Shivakumar, Compos. Struct. 84 (3) (2008) 271–281.
[3] W. Matthews, Defense News (2004) 32–35.
[4] G.N. Nurick, J.B. Martin, Int. J. Impact Eng. 8 (2) (1989) 171–186.
[5] T. Wierzbicki, G.N. Nurick, Int. J. Appl. Mech. 46 (1979) 899–918.
[6] Y. Lee, T. Wierzbicki, Int. J. Impact Eng. 31 (2005) 1253–1276.
[7] Y. Lee, T. Wierzbicki, Int. J. Impact Eng. 31 (2005) 1277–1308.
[8] V.H. Balden, G.N. Nurick, Int. J. Impact Eng. 32 (2005) 14–34.
[9] S.A. Tekalur, A. Shukla, K. Shivakumar, Compos. Struct. 84 (2008) 271–281.
[10] A.V. Amirkhizi, J. Isaacs, J. McGee, S. Nemat-Nasser, Phil. Mag. 86 (3) (2006) 5847–5866.
[11] C. Chen, D.G. Linzell, E. Alpman, L.N. Long, Tenth International Conference on Structures under Shock or Impact, 1–16 May, Portugal, 2008.
[12] C.M. Roland, D. Fragiadakis, R.M. Gamache, Compos. Struct. 92 (2010) 1059–1064.
[13] R.B. Bogoslovov, C.M. Roland, R.M. Gamache, Appl. Phys. Lett. (2007) 221910.
[14] A.J. Ryan, Polymer 31 (1989) 707.
[15] T. Elsayed, Constitutive Models for Polymers and Soft Biological Tissues, Ph.D. Dissertation, California Institute of Technology, 2007.
[16] C. Li, J. Lua, Mater. Lett. 63 (2009) 877–880.
[17] M. Grujicic, T. He, H. Marvi, B.A. Cheeseman, C.-F. Yen, J. Mater. Sci 45 (2010) 3136–3150.
[18] M. Grujicic, W.C. Bell, B. Pandurangan, T. He, J. Mater. Des. 31 (2010) 4050–4065.
[19] M. Grujicic, W.C. Bell, B. Pandurangan, P.S. Glomski, J. Mater. Eng. Perform., doi:10.1007/s11665-010-9724-z.
[20] C.M. Roland, R. Cassini, Polymer 48 (2007) 5747–5752.
[21] Y.A. Bahei-El-Din, G.J. Dvorak, O.J. Fredricksen, Int. J. Solids Struct. 43 (2006) 7644–7655.
[22] ABAQUS Version 6.8-1, User Documentation, Dassault Systems, 2008.
[23] M. Grujicic, G. Arakere, H. Nallagatla, W.C. Bell, I. Haque, J. Automobile Eng. 223 (2009) 301–325.
[24] M. Grujicic, W.C. Bell, G. Arakere, I. Haque, J. Automobile Eng. 223 (2009) 1419–1434.
[25] G.R. Johnson, W.H. Cook, Proceedings of the 7th International Symposium on Ballistics, 1983.
[26] G.R. Johnson, T.J. Holmquist, High Pressure Science and Technology, AIP, New York, 1994, 1993.
[27] M. Grujicic, B. Pandurangan, U. Zecevic, K.L. Koudela, B.A. Cheeseman, Multi-discipline Model. Mater. Struct. 3 (2007) 287–312.
[28] M. Grujicic, B. Pandurangan, N. Coutris, B.A. Cheeseman, C. Fountzoulas, P. Patel, Int. J. Impact Eng. 36 (2009) 386–401.
[29] M. Grujicic, B. Pandurangan, W.C. Bell, N. Coutris, B.A. Cheeseman, C. Fountzoulas, P. Patel, J. Mater. Eng. Perform. 18 (November (8)) (2009) 1012–1028.
[30] J. Yi, M.C. Boyce, G.F. Lee, E. Balizer, Polymer 47 (2006) 319–329.